On the Distribution of Carbon in Martensite

DAVID KALISH AND E. M. ROBERTS

The statistical-mechanics of a generalized perfect lattice gas is used to describe the distribution of interstitial solute atoms in martensite. In untempered martensite, partitioning of mobile interstitial carbon occurs between normal octahedral interstitial sites and those distorted sites around immobile dislocations. The statistics adopted acknowledge the finite number of each kind of site per unit volume of martensite. The dislocation density, fraction of twinned martensite, and the arrangement of dislocations are all input variables in the calculations. The principal quantities calculated are the fraction of carbon atoms segregated to dislocations and the fraction of distorted sites occupied as functions of the carbon content and substructure. The equilibrium distribution of carbon is also determined for tempering conditions where either ϵ-carbide or cementite may precipitate. Here, the change in the solubility limit of ferrite with dislocation density is predicted. In untempered low carbon martensites (at 300°K) 85 pct of the carbon will be segregated to dislocations at equilibrium. This value decreases to 60 pct in an 0.80 wt pct C steel. Less than 5 pct of the distorted sites are filled when the dislocation distribution is uniform. Much higher concentrations occur when the long range stresses of the dislocations are relaxed and the mean carbon/dislocation interaction energy increases. Analogous results are presented for the equilibrium among carbides, normal sites, and distorted sites. The predictions of the lattice gas model are in agreement with numerous independent experimental observations.

THE interstitial carbon (and nitrogen) content in martensitic steels markedly influences the flow strength and tempering process. In this regard, it is well-established that the substructure, *i.e.* the proportions of lath or twinned martensite, the dislocation density, and the degree of dislocation cell formation, is also significant in strengthening and tempering. These substructural parameters are commonly adjusted by alloying additions which alter the transformation behavior or by introducing plastic deformation into the heat treatment cycle.

The interaction of interstitial atoms with the substructure is really the key to understanding solid solution hardening in martensite and is an essential factor in determining the extent and morphology of precipitation during tempering. The question of the actual functional dependence of flow strength on carbon content obviously depends upon the distribution of carbon in martensite. Similarly, the appearance of iron carbides upon tempering involves a redistribution of carbon from one metastable equilibrium condition to another.

This paper develops a statistical-mechanical description of the distribution of interstitial solute atoms in a lattice containing dislocations. The conditions for thermodynamic equilibrium are then applied to the Fe-C system with a variety of substructures and tempering conditions. The quantitative predictions of equilibrium distributions are found to be in excellent agreement with independent experimental observations.

DAVID KALISH, formerly with Lockheed-Georgia Co., is now with Bell Telephone Laboratories, Atlanta, Ga. E. M. ROBERTS, formerly with Lockheed-Georgia Co., is now with Dames and Moore Co., Atlanta, Ga.

Manuscript submitted July 20, 1970.

THEORETICAL MODEL

Generalized Perfect Lattice Gas

As our model we choose that of a perfect lattice gas in which each solute atom may occupy one of a a specified set of lattice sites, with no more than one solute atom on a given site at any one time. The solute atoms are assumed not to interact with one another. The lattice gas is a successful model for several problems in chemical physics. Examples closely related to the present problem are the localized monolayer adsorption of a gas or liquid on a solid surface and the problem of clathrate solutions. In the theory of localized monolayer adsorption[1] it is usual to assume that all sites for adsorption are equivalent whereas in the theory of clathrate solutions,[2] it is necessary to account for the presence of more than one kind of adsorption site.

In order to apply the perfect lattice gas model to the Fe-C system, it is necessary to account for the presence of multiple types of lattice sites wherein the solute carbon atoms may reside. The generalization of the lattice gas to include the presence of several kinds of sites for a somewhat different problem has been given by Fowler.[1] This approach is adapted here to the case of interstitial solid solutions with the iron atoms being the host lattice and the carbon atoms serving as the adsorbed gas. Here, the sites are identified as the octahedral interstitial positions in the bcc iron lattice. Equations auxiliary to those used by Fowler are presented below.

It is assumed that bringing a carbon atom into an octahedral interstitial site of a type K changes the total energy of the atom by an additive amount λ_K without affecting the internal energy of the atom. With this simplification the single atom partition function for a site of type K is

$$q(\lambda_K) = \exp(\beta\lambda_K)q \quad [1]$$

where β is $1/(kT)$ and q is the partition function of the standard state for which $\lambda_K = 0$.

Fowler[1] has shown that in the discrete case the equilibrium number of solute atoms in the lattice is given by

$$N = \sum_K \frac{G_K z q_K}{1 + z q_K} \quad [2]$$

where z is the activity of the solute species and G_K is the number of type K sites. For the continuous case

$$N = \int \frac{zq(\lambda)}{1 + zq(\lambda)} f(\lambda) d\lambda \quad [3]$$

where $f(\lambda)$ is a distribution of sites over the range of absorption energy λ.

Within the framework of the present model, which neglects any change in the crystal due to the presence of solute atoms and neglects interactions between solute atoms, the choice of $f(\lambda)$ is independent of the statistical mechanics of the problem. Within broad limits of $f(\lambda)$ decreasing with increasing λ, the actual functional form of $f(\lambda)$ is *not critical* to the solution of the equilibrium conditions. For our numerical calculations we have chosen

$$f(\lambda) = AG \exp(-\alpha\beta\lambda), \quad \lambda_1 \leq \lambda \leq \lambda_2 \quad [4]$$
$$= 0, \text{ otherwise}$$

where A is a normalizing factor, G is the total number of sites in the range λ_1 to λ_2, α is a positive geometrical factor related to the mean value of the interaction energy, $\bar{\lambda}$, by

$$\bar{\lambda} = \frac{1}{G} \int_{\lambda_1}^{\lambda_2} \lambda f(\lambda) d\lambda \quad [5]$$

Equilibrium Between Two Lattices

The problem of partitioning solute carbon atoms between normal interstitial sites and stressed sites may be described by considering two lattices in thermal and material contact wherein the solute atoms may move freely from one crystal to the other. We may assume that the dislocation structure is stationary, *i.e.* there is no external applied stress and there is not sufficient thermal activation to induce recovery. The latter assumption applies to iron-carbon martensites up through the first stage of tempering. One lattice is then taken to be stress-free (no dislocations) and has G_0 interstitial sites. For a given activity:

$$\rho_0 = \frac{zq}{1 + zq} \quad [6]$$

The other lattice has all stressed sites, G_S of them, and $f(\lambda)$ is known. The condition for thermodynamic equilibrium is that the two lattices be at the same temperature and that the chemical potential of the solute atoms be equal in both lattices. The concentration of occupied sites in the stressed lattice is:

$$\rho_S = \frac{N_S}{G_S} \quad [7]$$

where N_S is calculated from Eq. [3]. The assumption of immobile dislocations means that G_0 and G_S are regarded as constants.

Several quantities of interest may now be calculated. The overall concentration of occupied sites is:

$$\rho_T = \frac{N_0 + N_S}{G_0 + G_S} \quad [8]$$

or

$$\rho_T = \frac{x\rho_0 + \rho_S}{1 + x} \quad [9]$$

where $x = G_0/G_S$ describes the relative sizes of the unstressed and stressed phases. It should be noted that G_0/G_S is arbitrary as far as the statistical mechanics is concerned, and merely defines some independent and physically determined state: *e.g.* G_0/G_S depends on the dislocation density which may be a function of the martensite transformation temperature range or the amount of plastic deformation of the martensite. The fraction of solute atoms that reside in stressed sites is:

$$\frac{N_S}{N_T} = \frac{\rho_0}{(1 + x)\rho_T} \quad [10]$$

where $N_T = N_0 + N_S$. Finally, the weight fraction of solute atoms at equilibrium is:

$$W = \frac{y\rho_T M_i}{y\rho_T M_i + M_l} \quad [11]$$

where y is the number of available interstitial sites per lattice atom and M_i and M_l are the atomic masses of the interstitial solute and lattice solvent atoms, respectively.

RESULTS AND DISCUSSION

The equilibrium distribution of interstitial carbon atoms in ferrite may be computed by using the physical conditions to specify T, λ_1, λ_2, λ, ρ_0, and G_0/G_S. The binding energy of carbon to a dislocation is conveniently described by a continuous distribution of energy levels due to the large number of stressed sites at various energy levels in a real polycrystalline material. This is an appropriate assumption since the interactions of the stress fields of dislocations, in tangles and in cell walls, will alter the precise binding energies that could be assigned to specific sites based on an elastic strain energy calculation[6] for an individual dislocation interacting with an individual interstitial atom. Further, the relaxation of the long range stresses as sites are filled with solute atoms also adds to the smearing effect of the distribution of energy levels. As a first approximation we let the binding energy be distributed as an exponential function, Eq. [4], although other forms that provide for a rapid increase in the number of sites as the energy level decreases may work as well. (In a subsequent section, this distribution is modified by allowing for further dislocations clustering and the associated elimination of shallow potential wells.)

To simplify matters, we assume all screw dislocations. If we had a certain fraction of edge dislocations, the number of octahedral sites providing more stable positions than normal sites would be reduced by $0.5 f_E$, where f_E is the fraction of edge dislocations. The decreased trapping capacity of edge dislocations, as compared to screws, is due to the unfavorable posi-

tions on the compression side of an edge dislocation[3] while all angular positions around a screw dislocation line contain favorable trapping positions. The maximum binding energy, λ_2, of carbon to screw dislocations is reported as 0.46 ev,[3] based on an elastic strain energy calculation, for a distance of one Burgers vector from the dislocation; 1.07 ev[4] based on atomic potentials within the dislocation core, or may be taken as 0.71 ev[5] by extending the usual hyperbolic energy-distance relation into the core with a simple sinusoidal force law. Experimental evidence supports the assumption of primary screw dislocations[6] and only relatively minor changes in the effective dislocation density, as is used here, would be required to account for a change in $f(\lambda)$ due to the presence of edge components. Initial calculations showed that the equilibrium distributions are *insensitive* to the value of λ_2, provided first that $\lambda_2 \gg KT$, and second that λ_1 and $\bar{\lambda}$ remain the same. Thus, for convenience we use $\lambda_2 = 0.71$ ev, with $\lambda = 0.46$ ev/r for $r \geq 1$b. The ratio G_0/G_S is equivalent to the ratio of planar areas normal to a dislocation which have sites less favorable and more favorable than λ_1. This is a simple geometric problem if one assumes a hyperbolic energy-distance relationship (for $r \geq 1$b).

Untempered Martensite

The first case to be examined is that of an as-quenched martensite which reaches a metastable equilibrium in terms of the solute carbon redistribution. This occurs upon aging at a temperature where carbon is mobile, such as above 215°K, but below the first stage of tempering where ϵ-carbide forms.

The substructure of Fe-C martensites will vary as a function of the alloy composition due to the decrease in the M_S temperature with increasing carbon content. As dislocation martensite is replaced by twinned martensite, the concentration of stressed interstitial sites will decrease. The fraction of twinned martensite is approximately:[7]

$$f_{tw} = 50.06 W_C - 0.063 \quad [12]$$

where W_C is the weight fraction of carbon. The minimum binding energy is set equal to the thermal energy, kT, at 300°K, *i.e.*, $\lambda_1 = 0.027$ ev. It follows, by dividing the planar area normal to the dislocation lines in half and by assuming the twinned martensite contains no stressed sites, that the mean energy, $\bar{\lambda}$, is equal to 0.038 ev. With a dislocation density of 10^{12} cm-disl per cu cm in the lath martensite, the equilibrium fraction of carbon atoms segregated to dislocations is given in Fig. 1 using Eq. [10]. In low carbon martensite, ≤0.2 wt pct C, about 85 pct of the carbon atoms are trapped by dislocations. This is in excellent agreement with resistivity measurements[7] which indicate that from 80 to 88 pct of the carbon, in this composition range, has segregated to dislocations or lath boundaries during quenching. Internal friction measurements indicate that about 90 pct of interstitial carbon is lost from solution (*i.e.* segregates to dislocations) when the dislocation density reaches 10^{11} per sq cm.[8] Further, Mössbauer spectroscopy of iron-carbon solid solutions has shown that at high solute concentrations, particularly in supersaturated martensites, carbon clusters very readily.[9] When the alloy composition is increased to 0.8 wt pct C, and the substructure contains 35 pct twinned martensite, there is still 66 pct of the carbon in stressed sites. (This condition is equivalent to reducing the dislocation density to 6.5 × 10^{11} cm-disl per cu cm in 100 pct lath martensite.) Higher twin concentrations will further reduce the percent of carbon in stressed sites. The distribution of carbon between stressed and unstressed sites is

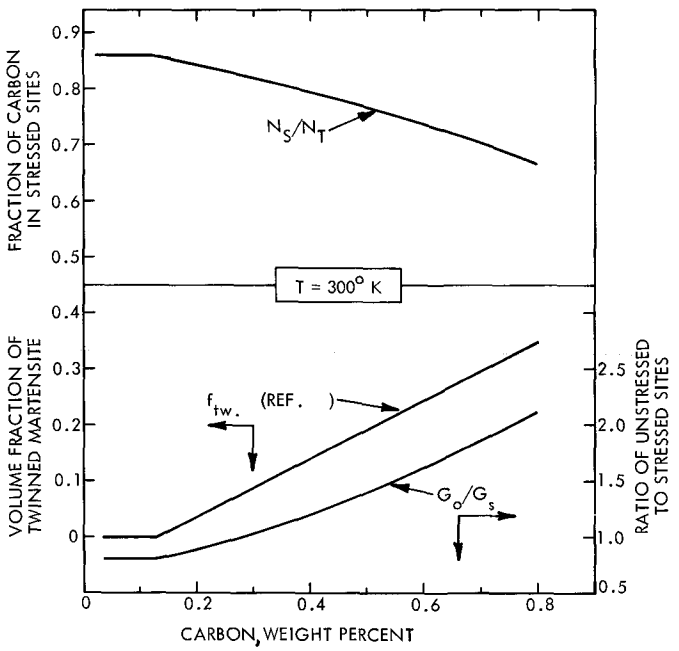

Fig. 1—Fraction of carbon atoms in stressed sites for mixtures of twinned and dislocation ($\rho_d = 10^{12}$ cm-disl per cu cm) martensite.

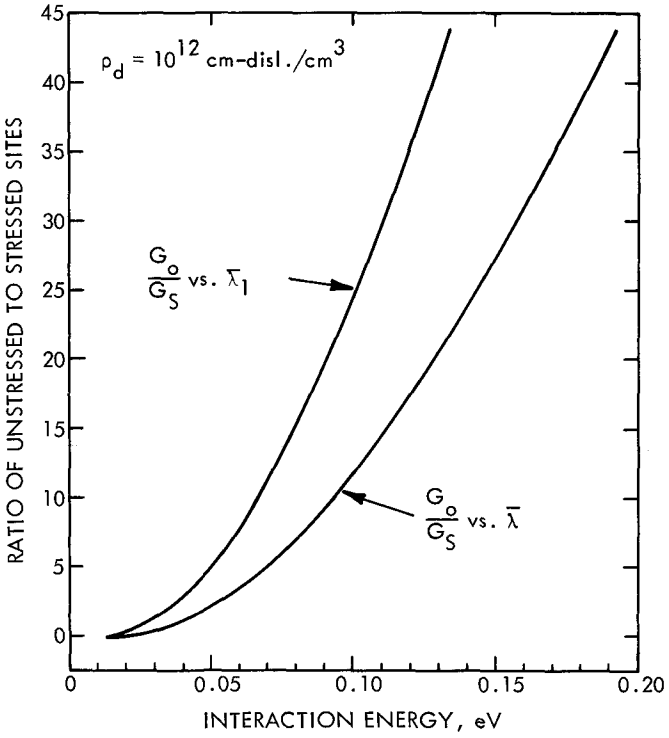

Fig. 2—Effect of increasing the minimum and mean interaction energies on the ratio of the unstressed to stressed sites at 300°K.

not significantly altered for temperatures between 225° and 400°K, assuming that the carbon is mobile within this temperature range. These results suggest that the high hardness of quenched plain carbon and alloy steels is associated with the rapid segregation of mobile carbon atoms to dislocations. The redistribution of the solute atoms from normal interstitial positions to the stressed sites can occur during conventional quenching,[7] and during aging at room temperature[10] prior to testing. As Cohen[11] has noted, the concept of cellular martensite hardening by individual contributions from dislocations and from interstitial carbon is relatively naive; the cross-effects being most important, since at the onset of testing most of the carbon is segregated to dislocations.

Next we examine the effect of reducing the number of low binding energy sites on the fraction of carbon atoms in stressed sites and on the fraction of stressed sites that are filled. The stressed sites relatively far from the dislocation may be eliminated due to mutual relaxation of the long-range stresses through clustering of dislocations and cell formation. Further, in special cases,[12] these long-range stresses may be relieved by the actual filling of other stressed sites close to the dislocation. An artificial dislocation clustering parameter may be constructed which preferentially eliminates the shallow potential wells by *constricting* the circular area normal to the dislocation line. Consequently, λ_1 and $\bar{\lambda}$ are increased, hand-in-hand, *without* changing λ_2, and the ratio of unstressed to stressed sites increases, Fig. 2. Clustering leads to fewer stressed sites but to an increase in the mean binding energy. Changing $\bar{\lambda}$ in this manner is equivalent to altering the geometrical shape factor α in Eq. [4].

The fraction of carbon atoms in stressed sites vs the carbon content and mean binding energy is given in Fig. 3, for a dislocation density of 10^{12} cm-disl per cu cm at 300°K. At the lower carbon contents, *e.g.* 0.2 wt pct C, as $\bar{\lambda}$ increases, N_s/N_t decreases due to the dominating effect of fewer stressed sites being available. However, as $\bar{\lambda}$ increases further, for $G_0/G_s > 1$, the $f(\lambda)$ function dominates and N_s/N_t rises with increasing $\bar{\lambda}$. In low carbon martensites with a well-developed cellular substructure, *i.e.* a high $\bar{\lambda}$, the fraction of carbon in stressed sites can exceed 90 pct. Eliminating shallow potential wells does not reduce the extent of segregation to the dislocations but serves to do just the opposite, since the equilibrium contribution with low concentrations of solute is dominated by $\bar{\lambda}$ and not by G_0/G_s. The fraction of carbon in stressed sites, in alloys up to 0.50 wt pct C, remains about 75 pct for all clustering conditions. For these compositions, the quantity of twinned martensite is small, Fig. 1, and will not significantly alter the results. The difference in percentage of carbon segregation to dislocations[7] of 94 pct from internal friction measurements at 300° to 400°K vs 85 pct from resistivity measurements at 77°K can be explained by more substructure relaxation in the former tests and an accompanying shift of $\bar{\lambda}$ to higher values.

Above 0.60 wt pct C, the concentration of stressed sites is the dominating factor at all values of $\bar{\lambda}$. Thus, N_s/N_t decreases with increasing $\bar{\lambda}$. The quantity of twinned martensite also becomes significant at those higher carbon levels and will cause a more rapid decrease in N_s/N_t with $\bar{\lambda}$ than for the dislocation martensites of Fig. 3.

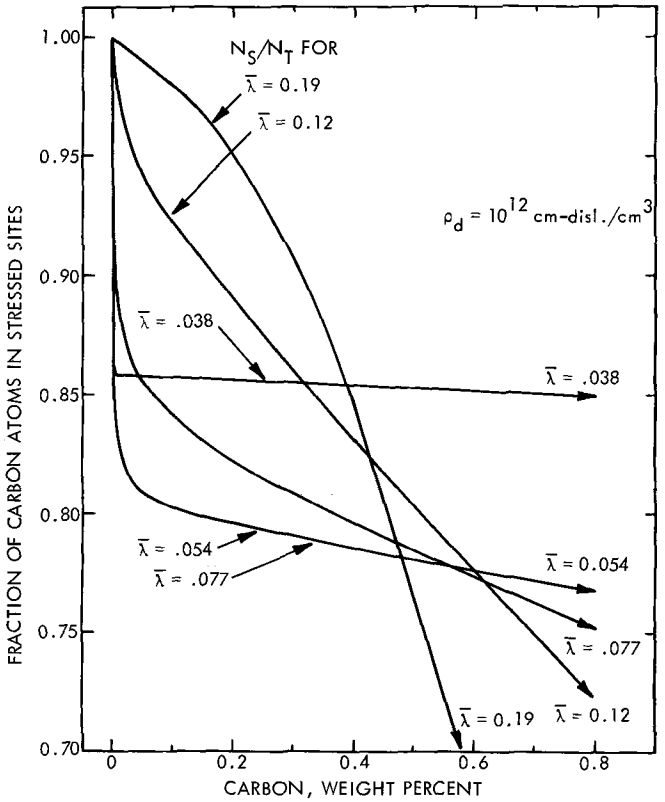

Fig. 3—Effect of dislocation clustering on the fraction of interstitial carbon atoms in stressed sites at 300°K.

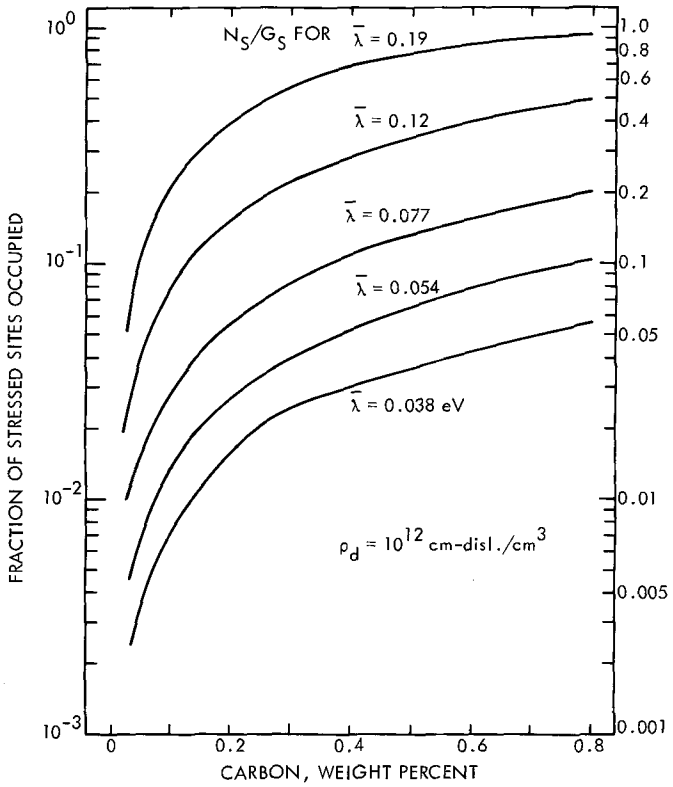

Fig. 4—Fraction of stressed sites occupied vs carbon content for various degrees of dislocation clustering at 300°K.

The effect of dislocation clustering on the equilibrium distribution of interstitial carbon in martensite may be alternatively depicted by the fraction of stressed sites occupied (N_s/G_s), Fig. 4, rather than by the fraction of solute in stressed sites (N_s/N_t), Fig. 3. In the absence of dislocation clustering ($\bar{\lambda}$ = 0.038 ev) more than 85 pct of carbon atoms reside in less than 6 pct of the stressed sites. The correction for twinned martensite formation will raise this value of N_s/N_t to about 9 pct. With extensive dislocation clustering ($\bar{\lambda}$ = 0.19 ev) in low carbon martensite ($\leq$ = 0.20 wt pct C) up to 40 pct of the stressed sites will be filled. When N_s/G_s exceeds about 40 pct there is a rapid decrease in N_s/N_t, Fig. 3, and the number of available stressed sites becomes the dominant term in the equilibrium distribution.

First Stage of Tempering

Tempering of conventionally hardened plain carbon and low alloy steels at temperatures of 425° to 500°K results in the formation of ϵ-carbide ($\sim Fe_{2.4}C$) if the martensite contains more than 0.20 to 0.25 wt pct C. It is well-documented that low carbon steels do not precipitate ϵ-carbide; the solute carbon atoms remain in solid solution up to the third stage of tempering where cementite forms.

The normal precipitation of ϵ-carbide particle in medium carbon steels can be eliminated by strain tempering.[13,14] Kalish and Cohen[10] proposed a model wherein the additional dislocations created by plastic deformation cause a redistribution of the interstitial carbon to relatively stable positions about dislocations so that ϵ-carbide does not form. Similarly, ϵ-carbide particles already formed may be induced to dissolve by strain-tempering.[10,14] On the other hand, the first stage of tempering can be extended to low carbon martensite if a partially twinned substructure forms during the martensite reaction; this is accomplished by depressing the M_s temperature through alloying with nickel.[15]

These experimental observations suggest that the solubility of carbon in ferrite is enhanced by dislocations not only at ambient temperatures but also up through the first stage of tempering.

In the absence of dislocations, the binding energy of carbon to ϵ-carbide may be estimated as 0.27 ev from calorimetric measurements.[16] Consequently, in the first stage of tempering there is a competition, for the carbon atoms, between the interstitial sites and ϵ-carbide. Within the interstitial sites there is a partitioning between the normal interstitial sites and those sites stressed by dislocations. Several assumptions are required in order to deal with the three-"phase" system consisting of unstressed sites, stressed sites, and precipitate particles, because the three-way equilibrium cannot be handled directly at this time.

First, we *assume* that the partitioning between the unstressed and stressed sites is described as for untempered martensite. However, λ_1 is now limited by the competition for carbon atoms between the stressed sites and the ϵ-carbide rather than by the thermal energy as in the untempered martensite. This leads to the *assumption* that the only effective stressed sites for trapping carbon are those with $\lambda \geq 0.27$ ev. Finally, the equilibrium between the unstressed sites and the ϵ-carbide is approximated by the solubility limit of carbon in ferrite as given by the iron-cementite metastable equilibrium phase diagram. This solubility limit is calculated to be 0.006 wt pct C at 425°K. This

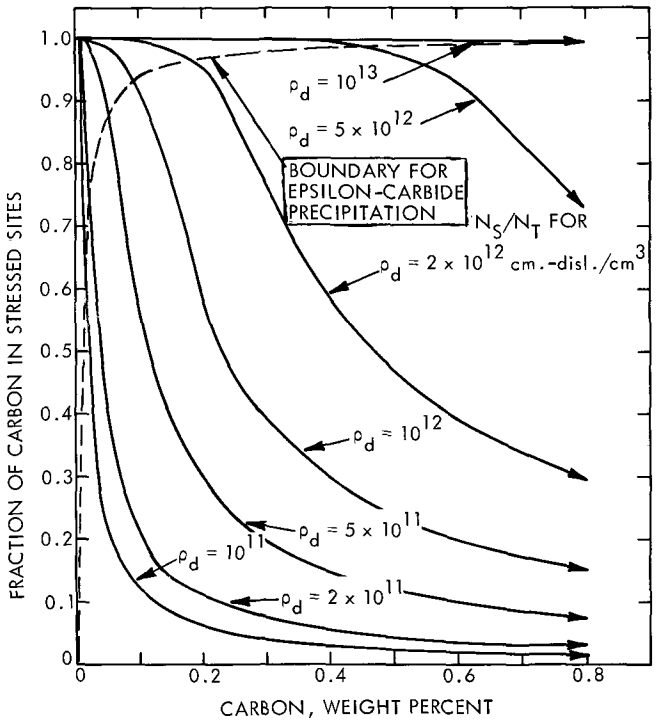

Fig. 5—Fraction of interstitial carbon in stressed sites vs carbon content and dislocation density for martensite tempered at 425°K.

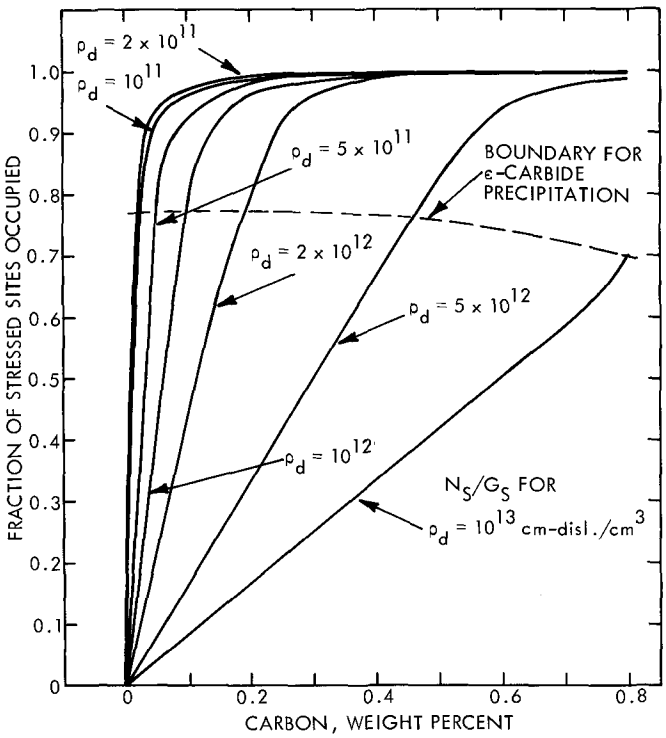

Fig. 6—Fraction of stressed sites occupied vs carbon content for a range of dislocation densities at 425°K.

value is obtained by modifying the equation[17] for the equilibrium limit in the presence of cementite, by using the heat of solution of ϵ-carbide in place of that for cementite.

The fraction of carbon in stressed sites, N_s/N_t, as a function of carbon content for various dislocation densities at 425°K is given in Fig. 5. The solid curves in Fig. 5, computed for $\lambda_2 = 0.71$ ev, $\lambda_1 = 0.27$ ev, and $\bar{\lambda} = 0.38$ ev, do not recognize the presence of ϵ-carbide other than by the values of λ_1 and $\bar{\lambda}$. The assumption as to the solubility limit of the unstressed ferrite is now employed. The condition for ϵ-carbide precipitation is given by $(1 - N_s/N_c)\, W_c > 6 \times 10^{-5}$, and is shown by the dashed curve in Fig. 5. For a particular dislocation density, if the carbon content exceeds this boundary then ϵ-carbide particles will form. Consequently, we find that about $\rho_d = 2 \times 10^{12}$ cm-disl per cu cm will completely suppress ϵ-carbide precipitation in martensite with up to 0.20 wt pct C; this is a reasonable dislocation density for lath martensites. It follows that increasing ρ_d by plastic deformation, to 5×10^{12} cm-disl per cu cm can suppress ϵ-carbide with up to 0.40 wt pct C, as has been observed.[14] But $\rho_d = 10^{13}$ cm-disl per cu cm is required to avoid ϵ-carbide in an 0.80 wt pct C martensite. The observation that strain tempering of such a high carbon martensite[14] only partially suppresses ϵ-carbide formation may be attributed to the inability to achieve the required dislocation density in a partly twinned substructure. In contrast, ϵ-carbide will readily form in a 0.11 wt pct C martensite[15] if the M_s temperature is lowered by alloying so that half of the substructure is twinned martensite.

The fraction of stress sites occupied, $\lambda \geq 0.27$ ev, upon tempering at 425°K is given in Fig. 6. The concentration of carbon segregated to dislocations proves to be considerably higher than at 300°K. The upper limit for N_s/G_s is about 0.77, the dashed curve in Fig. 6, in low carbon martensites and this limit decreases slightly to about 0.70 in an 0.80 wt pct C martensite. For a given dislocation density, as the carbon content increases the fraction of stressed sites occupied will increase, along one of the solid curves in Fig. 6, until the saturation concentration, Fig. 5, is exceeded and then ϵ-carbide will precipitate. We must keep in mind that the conditions depicted by Figs. 5 and 6 are approximate equilibrium distributions. The kinetics for reaching equilibrium are not implied, although the processes involved are likely to be rapid due to the high mobility of carbon at the temperatures in question. Further, the microstructure may go through some transition arrangements in striving to reach equilibrium at 425°K. For example, the carbon sitting in shallow potential wells and unstressed sites at 300°K may cluster and start to form ϵ-carbide nuclei as the tempering temperature is raised. However, some or all of these nuclei redissolve at 425°K as the equilibrium is established among the stressed sites, unstressed sites, and precipitating particles. Furthermore, we can account for the resolution of initially formed ϵ-carbide particles by straining and further tempering.[10] Increasing the dislocation density at a given carbon content involves transferring from a curve about the boundary for ϵ-carbide precipitation, Fig. 6, to a curve below the boundary.

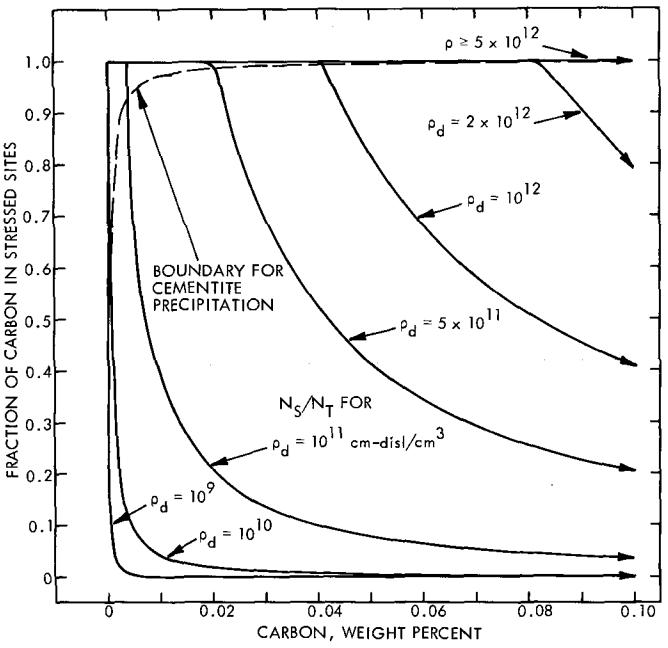

Fig. 7—Fraction of interstitial carbon in stressed sites vs carbon content and dislocation density for martensite tempered at 525°K.

Third Stage of Tempering

Tempering at 525°K, or above, results in the precipitation of cementite (Fe_3C) or a defect form of this carbide.[7] In addition, the dislocations become mobile and the total dislocation density begins to decrease by annihilation processes. Again, a kinetic description of the partitioning of carbon among stressed sites, normal sites, and cementite, while the dislocation structure is changing, is a formidable problem. The best approach at this time is to calculate a series of equilibrium situations based upon fixed dislocation densities. The carbon atoms may be partitioned among the three "phases" in a manner analogous to the first stage of tempering.

The equilibrium between G_0 and G_s sites is described as for untempered martensite. Now we allow only one site, per iron-atom plane intersected by a dislocation line, to participate in solute atom trapping. The site is the innermost interstitial position where $\lambda_1 = \lambda_2 = \bar{\lambda} = 0.71$ ev. All other positions where $\lambda \leq 0.5$ ev offer less favorable positions for carbon than the precipitating carbide with a binding energy for carbon of near 0.5 ev.[17] The equilibrium solubility limit between the unstressed sites and cementite at 525°K is 0.0003 wt pct C.[17]

The fraction of carbon in stressed sites as a function of carbon content and dislocation density is given by the solid curves in Fig. 7. The boundary condition for cementite precipitation, indicated by the dashed curve, is determined by N_0/G_0 reaching 3×10^{-4} wt pct C. It is not possible to significantly inhibit cementite precipitation by the presence of dislocations in most martensites.[10] Although there may be a kinetic effect if the cementite is forming from complexed carbon at dislocations as in deformed martensite rather than from ϵ-carbide.

However, the strength of strain-hardened ferrite

may be influenced by the segregation of carbon to cell walls.[18] Consider a heavily cold-worked ferrite with a cell structure consisting of perhaps 5×10^{12} disl-cm per cu cm in the cell walls, but the cell walls occupy only 10 pct of the volume of material. The effective ρ_d is 5×10^{11}, Fig. 7, and up to 0.02 wt pct C could be trapped at 525°K, with 98 pct of the carbon residing in dislocation core sites. Along these lines, the rate of flow strength increase, with a linear decrease in the cell size of ferrites, is known to depend upon the carbon content. We may now attribute this observation to an increase in the interstitial strengthening of the cell walls in going from 0.001 wt pct[19] to 0.007 wt pct C.[18] The results in Fig. 7 show that essentially all of the carbon present in these low carbon ferrites will redistribute to cell walls upon initial strain hardening. The ability of a cell wall to retain the freshly created dislocations and then to act as a barrier to further flow upon retesting will be dependent upon the interstitial strengthening. If the flow strength of the ferrites containing a distinct cell structure is reflected by the cell wall strength, then the interstitial hardening contribution is really magnified by a factor proportional to the reciprocal of the volume fraction of cell wall material.

The total interstitial carbon content, consisting of solute atoms in stressed as well as normal sites, may be combined to give an effective solubility limit of ferrite with respect to cementite. This solubility limit as a function of dislocation density is shown in Fig. 8 for 525°K. The increase in ρ_0 with temperature[17] would result in a shift of the curve in Fig. 8 towards the upper left; *i.e.*, at a higher temperature a given dislocation density would produce a higher solubility limit. Rudee and Huggins[20] predicted a similar result based upon a counting method that does not limit the number of sites. The true physical situation must account for a decrease in the dislocation density (and thus in specific number of sites) as the tempering proceeds with increasing temperature. The competing effect of decreasing G_S will dominate over the increased solubility due to a rise in temperature, and the net solubility limit will actually decrease as tempering continues in the third stage.

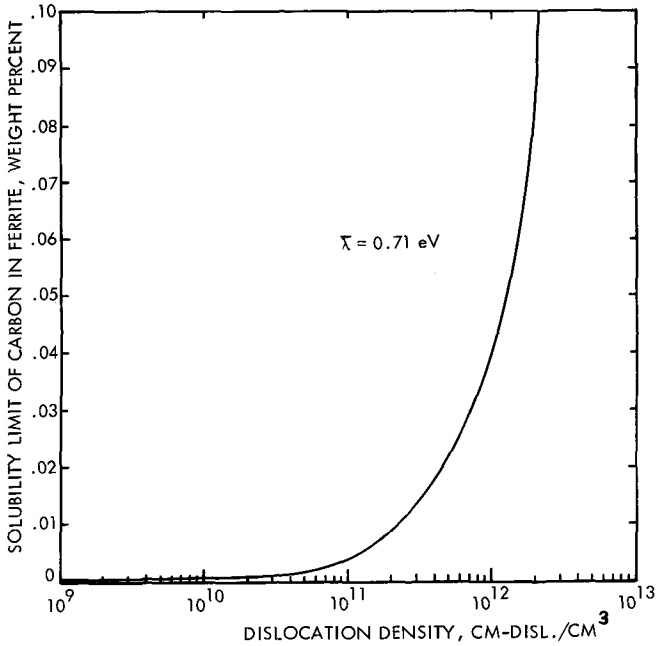

Fig. 8—Solubility limit of carbon in ferrite with respect to cementite at 525°K vs dislocation density.

CONCLUSIONS

1) The statistical mechanics of a generalized perfect lattice gas provides a successful model for describing the metastable equilibrium distribution of carbon in martensite at various stages of tempering. In untempered martensite, the solute carbon is partitioned between the distorted (or stressed) interstitial sites around dislocations and the normal (or unstressed) sites. Upon tempering at temperatures where carbides tend to form, the partitioning must include the appropriate carbide as a third sink for carbon.

2) Several important strengthening and microstructural effects may be attributed to the quantitative predictions of the lattice gas model.

3) In an untempered lath martensite, about 85 pct of interstitial carbon will be segregated to dislocations at equilibrium. This number decreases as the substructure becomes partly twinned, due to a lowering of the M_S temperature, but remains as high as 66 pct in an 0.8 wt pct Fe-C martensite.

4) The dislocation arrangement in martensite has a pronounced effect on the distribution of carbon. In low carbon martensites the relaxation of long-range stresses, by dislocation rearrangement, increases the segregation of solute to dislocations due to the dominating effect of an increase in the mean carbon/dislocation interaction energy. At high carbon levels, the decrease in the actual concentration of distorted interstitial sites dominates over the rise in the mean interaction energy, and so the fraction of carbon distributed to dislocations decreases. However, at all carbon levels, the concentration of carbon at dislocations will increase as the proportion of shallow potential wells decreases.

5) The appearance of ϵ-carbide in the first stage of tempering is controlled by the solubility limit of the ferrite, which, in turn, is influenced directly by the dislocation density. ϵ-carbide will not form until 70 to 77 pct of those interstitial sites (near the dislocation line) are filled which have a higher attraction for carbon than does ϵ-carbide. Deformation or alloying may be used to change the dislocation density, and thereby alter the carbon content at which ϵ-carbide may form.

6) Dislocations cannot trap an appreciable amount of carbon in competition with cementite in tempered martensite. However, in supersaturated cold-worked ferrites, well over 90 pct of the carbon will segregate to cell walls. The solubility limit of ferrite with respect to cementite will increase as the dislocation density is increased.

ACKNOWLEDGMENT

The authors wish to thank Mr. C. Stone for his assistance in the computations. This work was performed under an Independent Research Authorization of the Lockheed-Georgia Company.

REFERENCES

1. R. H. Fowler: *Statistical Mechanics,* Cambridge Univ. Press, London, 1936.
2. J. H. van der Waals and J. C. Platteeuw: *Advances in Chemical Physics,* Vol. II, Chap. 1, Interscience Publ., Inc., New York, 1959.
3. A. W. Cochardt, G. Schoek, and H. Wiedersich: *Acta Met.,* 1955, vol. 3, p. 533.
4. R. Chang: *Fundamental Aspects of Dislocation Theory,* Nat. Bur. Stand., Spec. Publ. 317, 1970.
5. David Kalish and Morris Cohen: IMD Symp. on *Strength and Deformation of Martensite,* May 5, 1969, Pittsburgh, Pa.; Lockheed-Georgia Company Research Memorandum, ER-11028, 1971.
6. H. D. Soloman and C. J. McMahon, Jr.: *Work Hardening,* p. 311, Gordon and Breach Science Publ., New York, 1968.
7. (a) G. R. Speich: *Trans. TMS-AIME,* 1969, vol. 245, p. 2553.
   (b) G. R. Speich: U.S. Steel Corp., Research Center, Monroeville, Pa., private communication, 1969.
8. J. M. Genin and P. A. Flinn: *Trans. TMS-AIME,* 1968, vol. 242, p. 1419.
9. J. C. Swartz: *Mater. Sci. Eng.,* 1969-70, vol. 5, p. 30.
10. David Kalish and Morris Cohen: *Mater. Sci. Eng.,* 1970, vol. 6, p. 156.
11. Morris Cohen: *Proc. of the Intern. Conf. on the Strength of Metals and Alloys,* Tokyo, 1967, Suppl. to *Trans. JIM,* 1968, vol. 9, p. xxiii.
12. J. P. Hirth and J. Lothe: *Theory of Dislocations,* Chap. 14, McGraw-Hill Book Co., New York, 1968.
13. D. V. Wilson: *Acta Met.,* 1955, vol. 5, p. 293.
14. B. A. MacDonald: Ph.D. Thesis, M.I.T., Cambridge, Mass., 1964.
15. C. J. Barton: *Acta Met.,* 1969, vol. 17, p. 1085.
16. R. A. Arndt and A. C. Damask: *Acta Met.,* 1964, vol. 12, p. 341.
17. L. Darken and R. Gurry: *Physical Chemistry of Metals,* McGraw Hill, New York, 1953.
18. G. Langford and Morris Cohen: *Trans. ASM,* 1969, vol. 62, p. 623.
19. H. J. Rack and Morris Cohen: *Mater. Sci. Eng.,* 1970, vol. 6, p. 320.
20. M. L. Rudee and R. A. Huggins: *Acta Met.,* 1964, vol. 12, p. 501.